

Long-working-distance fluorescence microscope with high-numerical-aperture objectives for variable-magnification imaging in live mice from macro- to subcellular

Hiroaki Kimura

AntiCancer, Incorporated
7917 Ostrow Street
San Diego, California 92111

and
University of California, San Diego
Department of Surgery
200 West Arbor Drive
San Diego, California 92103-8220
and
Kanazawa University
Graduate School of Medical Sciences
Department of Orthopaedic Surgery
Kanazawa, Ishikawa, Japan

Masashi Momiyama

AntiCancer, Inc.
7917 Ostrow Street
San Diego, California 92111

and
University of California, San Diego
Department of Surgery
200 West Arbor Drive
San Diego, California 92103-8220
and
Yokohama City University
Department of Gastroenterological Surgery
Graduate School of Medicine
3-9 Fukuura, Kanazawa-ku
Yokohama 236-0004, Japan

Katsuro Tomita

Hiroyuki Tsuchiya

Kanazawa University
Graduate School of Medical Sciences
Department of Orthopaedic Surgery
Kanazawa, Ishikawa, Japan

Robert M. Hoffman

AntiCancer, Incorporated
7917 Ostrow Street
San Diego, California 92111

and
University of California, San Diego
Department of Surgery
200 West Arbor Drive
San Diego, California 92103-8220

1 Introduction

Fluorescent protein expression has enabled the new field of *in vivo* cell biology.^{1,2} For example, we have engineered dual-color fluorescent cancer cells with one color in the nucleus

Abstract. We demonstrate the development of a long-working-distance fluorescence microscope with high-numerical-aperture objectives for variable-magnification imaging in live mice from macro- to subcellular. To observe cytoplasmic and nuclear dynamics of cancer cells in the living mouse, 143B human osteosarcoma cells are labeled with green fluorescent protein in the nucleus and red fluorescent protein in the cytoplasm. These dual-color cells are injected by a vascular route in an abdominal skin flap in nude mice. The mice are then imaged with the Olympus MVX10 macroview fluorescence microscope. With the MVX10, the nuclear and cytoplasmic behavior of cancer cells trafficking in blood vessels of live mice is observed. We also image lung metastases in live mice from the macro- to the subcellular level by opening the chest wall and imaging the exposed lung in live mice. Injected splenocytes, expressing cyan fluorescent protein, could also be imaged on the lung of live mice. We demonstrate that the MVX10 microscope offers the possibility of full-range *in vivo* fluorescence imaging from macro- to subcellular and should enable widespread use of powerful imaging technologies enabled by genetic reporters and other fluorophores. © 2010 Society of Photo-Optical Instrumentation Engineers. [DOI: 10.1117/1.3526356]

Keywords: green fluorescent protein; red fluorescent protein; mice; subcellular imaging; fluorescence microscopy; *in vivo* cell biology.

Paper 10446R received Aug. 9, 2010; revised manuscript received Oct. 13, 2010; accepted for publication Oct. 29, 2010; published online Dec. 23, 2010.

and another in the cytoplasm that enable real-time nuclear-cytoplasmic dynamics to be visualized in living cells *in vivo* as well as *in vitro*. To obtain the dual-color cells, red fluorescent protein (RFP) was expressed in the cytoplasm of cancer cells, and green fluorescent protein (GFP) linked to histone H2B

Address all correspondence to: Robert M. Hoffman, Ph.D., AntiCancer Inc., 7917 Ostrow Street, San Diego, California, 92111, Tel: 858-654-2555, Fax: 858-268-4175, E-mail: all@anticancer.com.

was expressed in the nucleus. Nuclear GFP expression enabled visualization of nuclear dynamics, whereas simultaneous cytoplasmic RFP expression enabled visualization of nuclear cytoplasmic ratios as well as simultaneous cell and nuclear shape changes. Thus, total cellular dynamics can be visualized in living dual-color cells in real time.

The cell cycle position of individual living cells was readily visualized by the nuclear-cytoplasmic ratio and nuclear morphology. Real-time induction of apoptosis was observed by nuclear size changes and progressive nuclear fragmentation. Mitotic cells were visualized by whole-body imaging after injection in the mouse ear.^{3,4}

Oscillating proteins that mark cell-cycle transitions were linked with RFP or GFP, respectively, to label individual G1-phase cells red and S/G2/M phase cells green. Cell cycle position can now also be visualized *in vivo* with such fluorescent protein labeling.⁵

Opening a reversible skin flap in the light path markedly reduces signal attenuation, increasing detection sensitivity manyfold. The observable depth of tissue is thereby greatly increased, enabling the visualization of single fluorescent protein-labeled cells deeply within the animal. With the skin-flap window, single cancer cells could easily be visualized on internal organs such as the brain, liver, and pancreas.⁶

We noninvasively imaged cancer cell/stromal cell interaction in the tumor microenvironment and drug response at the cellular and subcellular levels in live animals in real time. GFP-expressing mice were transplanted with the dual-color cancer cells labeled with GFP in the nucleus and RFP in the cytoplasm. In this model, drug response of both cancer and stromal cells in the intact live animal were imaged in real time. Various *in vivo* phenomena of tumor-host interaction and cellular dynamics were imaged, including mitotic and apoptotic tumor cells, stromal cells interacting with the tumor cells, tumor vasculature, and tumor blood flow.⁷

Using the dual-color cancer cells already described, we observed the nuclear and cytoplasmic behavior of cancer cells in real time in blood vessels as they trafficked by various means or adhered to the vessel surface in an abdominal skin flap. During extravasation, real-time dual-color imaging showed that cytoplasmic processes of the cancer cells exited the vessels first, with nuclei following along the cytoplasmic projections. Both cytoplasm and nuclei underwent deformation during extravasation. Different cancer cell lines seemed to strongly vary in their ability to extravasate.⁸

The results just described demonstrate the great potential of *in vivo* imaging based on fluorescent proteins. These studies enabled the founding of the field of *in vivo* cell biology and mostly used a complex imaging system, the OV100 (Olympus Corp., Tokyo, Japan), which is no longer commercially available.¹ What is currently needed is an appropriate, simpler, and more accessible and economic imaging system that can take advantage of this technology so that *in vivo* cell biology can be widely practiced.

In this paper, we investigate how a long-working-distance fluorescence microscope, with high-numerical-aperture objectives for variable-magnification imaging in live mice, from macro- to subcellular, can fulfill this need for widespread investigations of *in vivo* cell biology.

2 Materials and Methods

2.1 Establishment of Dual-Color Cancer Cell Lines

To establish the human osteosarcoma 143B dual-color cell line, in which GFP is expressed in the nucleus and RFP is expressed in the cytoplasm, the cells were transfected with retroviral DsRed2 and H2B-GFP vectors. In brief, the *HindIII/NotI* fragment from pDsRed2 (Clontech Laboratories, Inc., Palo Alto, California), containing the full-length RFP cDNA (complementary DNA), was inserted into the *HindIII/NotI* site of pLNCX2 (Clontech Laboratories, Inc.) containing the neomycin resistance gene. PT67, an NIH3T3-derived packaging cell line (Clontech Laboratories, Inc.), expressing the 10 A1 viral envelope, was cultured in Dulbecco modified Eagle medium (DMEM; Irvine Scientific, Santa Ana, California) supplemented with 10% heat-inactivated fetal bovine serum (FBS; Gemini Bio-products, Calabasas, California). For vector production, PT67 cells were incubated with a precipitated mixture of LipofectAMINE reagent (Life Technologies, Inc. Grand Island, New York) and saturating amounts of pLNCX2-DsRed2 plasmid for 18 h. The cells were examined by fluorescence microscopy 48 h post-transfection. For selection of clones producing high amounts of an RFP retroviral vector (PT67-DsRed2), the cells were cultured in the presence of 200 to 1000 $\mu\text{g/ml}$ G418 (Life Technologies, Inc.) increased stepwise over 7 days.

The histone H2B gene has no stop codon, thereby enabling the ligation of the H2B gene to the 5'-coding region of the GFP gene (Clontech Laboratories, Inc.). The histone H2B-GFP fusion gene was then inserted at the *HindIII/CaII* site of the pLHCX (Clontech Laboratories, Inc.) that has the hygromycin resistance gene. To establish a packaging cell clone producing high amounts of histone H2B-GFP retroviral vector, the pLHCX histone H2B-GFP plasmid was transfected in PT67 cells using the same methods already described for PT67-DsRed2. The transfected cells were cultured in the presence of 200 to 400 $\mu\text{g/ml}$ G418 (Life Technologies, Inc.) increased stepwise over 7 days.

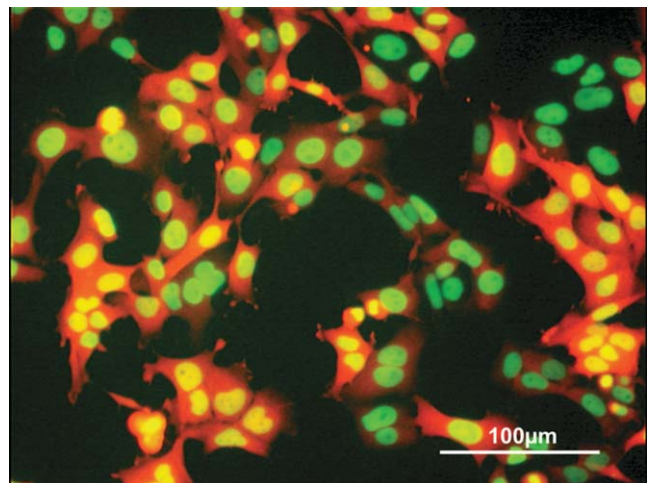


Fig. 1 Dual-color cancer cells. Human 143B osteosarcoma cells expressing GFP in the nucleus and RFP in the cytoplasm *in vitro*. All cells in the population express both GFP and RFP, indicating stability of both transgenes. See Sec. 2 for details.

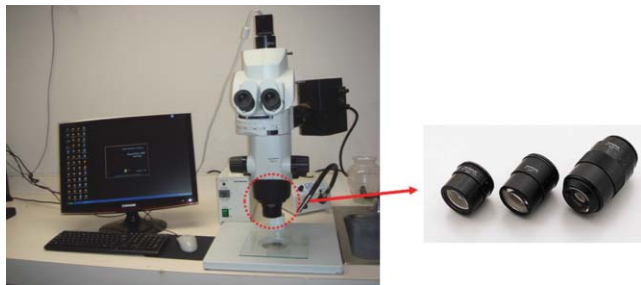


Fig. 2 Olympus MVX10 Macro view with FluorVivo Mag imaging system and FluoCam 1500G color CCD camera. Specially designed 0.63 \times , 1 \times , and 2 \times planapochromatic objectives with high-numerical-apertures (NAs; see Sec. 2 for details) are shown. All three objectives are pupil-corrected for optimal image flatness and show high transmission and superior chromatic aberration correction.

To establish 143B dual-color cells, clones of these cells expressing RFP in the cytoplasm were initially established. In brief, cells were incubated with a 1:1 precipitated mixture of retroviral supernatants of PT67-RFP cells and RPMI (Roswell Park Memorial Institute) 1640 medium (Irvine Scientific, Santa Ana, California) containing 10% FBS for 72 h. Cells were harvested with trypsin/EDTA 72 h post-transduction and subcultured at a ratio of 1:15 into selective medium, which contained 200 $\mu\text{g}/\text{ml}$ G418. The level of G418 was increased stepwise up to 800 $\mu\text{g}/\text{ml}$. RFP cells were then incubated with a 1:1 precipitated mixture of retroviral supernatants of PT67 H2B-GFP cells and culture medium. To select the double transformants, cells were incubated with hygromycin 72 h after transfection. The level of hygromycin was increased stepwise from 200 to 800 $\mu\text{g}/\text{ml}$ (Fig. 1).

2.2 Long-Working-Distance Variable-Magnification Fluorescence Microscope for In Vivo Imaging

The Olympus MVX10 Macro View (OLYMPUS Corporation; Center Valley, Pennsylvania) and a FluoCam 1500G color CCD camera were used for imaging in live mice (Fig. 2).

The FluoCam 1500G is a digital color CCD camera manufactured to the specifications of INDEC Systems, Inc. (Santa Clara, CA). It is based on a Sony ICX285 sensor and has 1392 \times 1040 pixels, each 6.45 mm^2 . Its quantum efficiency is over 60%. It supports real-time imaging at rates greater than 20 images/sec.

The Olympus MVX10 MacroView employs a single-zoom optical path with a large diameter, which is optimized to collect light with unprecedented efficiency and resolution at all magnifications while still using the 2-position revolving nosepiece.

Table 1 Objective lenses that can be used with the MVX10.

Lens Designation and Magnification	NA	WD
MVPLAPO 0.63 \times	NA 0.15	WD 87 mm
MVPLAPO 1 \times	NA 0.25	WD 65 mm
MVPLAPO 2 \times C	NA 0.5	WD 20 mm

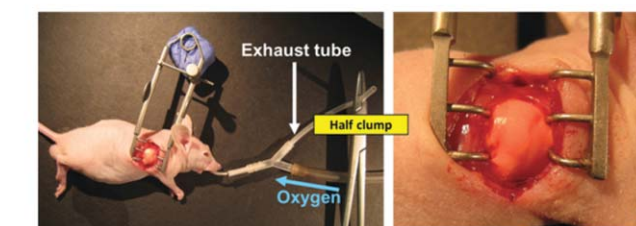
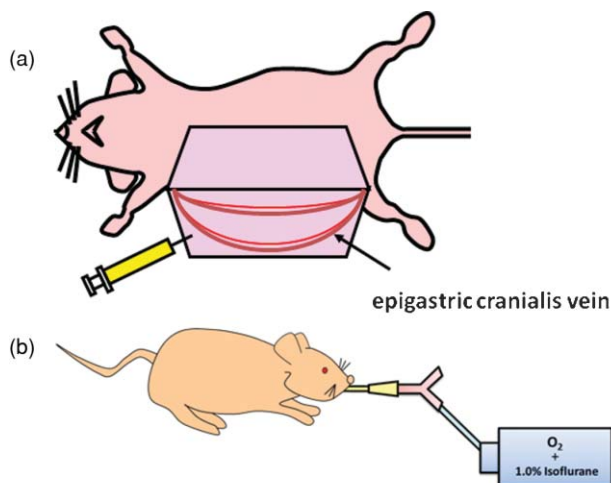


Fig. 3 (a) Mouse skin flap model for imaging nuclear-cytoplasmic dynamics of cancer cells. An arc-shaped incision was made in the abdominal skin of nude mice. The sc connective tissue was separated to free the skin flap without injuring blood vessels. Cancer cells were then injected into the proximal site of the epigastrica cranialis vein. Trafficking cancer cells in blood vessel can be imaged. See Sec. 2 for details. (b) Model for imaging single cancer cells in the lung. To visualize lung metastatic colonies or cells in the lung at the microlevel, the lung surface of live mice was directly imaged. A thoracotomy was performed to expose the lungs. For the animal to breathe with an open chest wall, an intubation tube was tied to a Y-type connector and an exhaust tube was attached to one of the ends. The oxygen tube was connected to a Y-shaped connector. The chest cavity was then opened. To maintain anesthesia throughout the procedure, an inhalant anesthesia system was used. The oxygen flow rate was set at 100 cc/min. The vaporizer was set at 1.0% isoflurane per volume of oxygen. To control inflation of the lung, the exhaust tube was half clamped. Adjusting air pressure enabled the lung to inflate to the proper fullness.⁹

The 0.63 \times and 2 \times objectives expand the usable zoom range up to 31. The objectives are parfocal corrected, making refocusing after objective switching very quick and easy. Only a small amount of fine focusing is necessary to return to the optimal focus position, making macro- to microchanges seamless. The 2 \times objective is also equipped with an additional correction collar to adjust the image quality independently of the specimen medium. This microscope enables fluorescence imaging of whole organisms in a range from low magnification to the detailed observation at the cellular level at high magnification. See Table 1.

In comparison with currently-available microscopes, the MVX10 provides a long-working-distance and a much higher NA. This makes variable-magnification fluorescence imaging especially powerful, improves speed and precision, and eliminates the necessity to switch back and forth between a stereomicroscope and an inverted microscope.

2.3 Mouse Skin-Flap Model for Imaging Real-Time Nuclear-Cytoplasmic Dynamics of Trafficking Cancer Cells In Vivo

To image nuclear-cytoplasmic dynamics of trafficking cancer cells in real time in live mice, dual-color cancer cells, expressing GFP in the nucleus and RFP in the cytoplasm, were injected into the epigastric cranialis vein.⁸ Nude mice were anesthetized with a ketamine mixture (10 μ L ketamine HCL, 7.6 μ L xylazine, 2.4 μ L acepromazine maleate, and 10 μ L H₂O) via subcutaneous (sc) injection. An arc-shaped incision was made in the abdominal skin. The sc connective tissue was separated to free the skin flap without injuring the epigastric cranialis artery and vein. The skin flap was spread and fixed on the flat stand. A total of 30 μ L medium containing 5×10^5 143B dual-color cells were injected into the epigastric cranialis vein. For imaging cancer-cell trafficking in blood vessels, images were acquired 1 h after injection [Fig. 3(a)].

2.4 Lung Metastasis Imaging with Dual-Color Fluorescent Cells

To visualize lung metastatic colonies in live mice, a total of 200 μ L medium containing 2×10^6 143B dual-color cells were injected into the tail vein of nude mice. Two weeks after injection, we imaged the lung surface of live mice directly. In brief, the mouse was anesthetized and intubated with an intravenous catheter (SURFLO®, 20 gauge, 25 mm length; Terumo Medical Corporation, Elkton, Maryland) as an endotracheal tube. The intubation tube was attached and tied to a Y-type connector, which was connected, to an inhalant anesthesia system, PAM (Portable Anesthesia Machine, Summit Anesthesia Solutions, Bend, Oregon). A 5-cm exhaust tubing was attached to one end of the Y-shaped connector. The carrier gas was 100% oxygen, and the vaporizer was set at 1.0% isoflurane (Isothesia, Butler Animal Health Supply, Dublin, Ohio) per volume of oxygen. The chest wall was then opened, and an exhaust tube was half clamped to inflate the lung. By adjusting the air pressure, the lungs were inflated to the proper fullness to mimic its natural condition and optimally image the lung metastases⁹ [Fig. 3(b)].

3 Results and Discussion

3.1 Imaging of Dual-Color Cancer Cells in Capillaries of Live Mice

We imaged cancer cell trafficking at the subcellular level in live mice, using the MVX10 microscope. A skin flap was made without injuring the epigastric cranialis artery and vein and then spread and fixed on a stand. Cancer cells were then injected into this vein. Individual cells could then be easily visualized in capillaries and in microvessels in the skin in the live mouse with the MVX10 (Fig. 4 and Video 1). The wired epigastric cranialis vein was filled with round cancer cells. Some cells were moving, some were trapped due to size restriction in capillaries, where the cells and nuclei were highly deformed, depending on the diameter of the vessel.

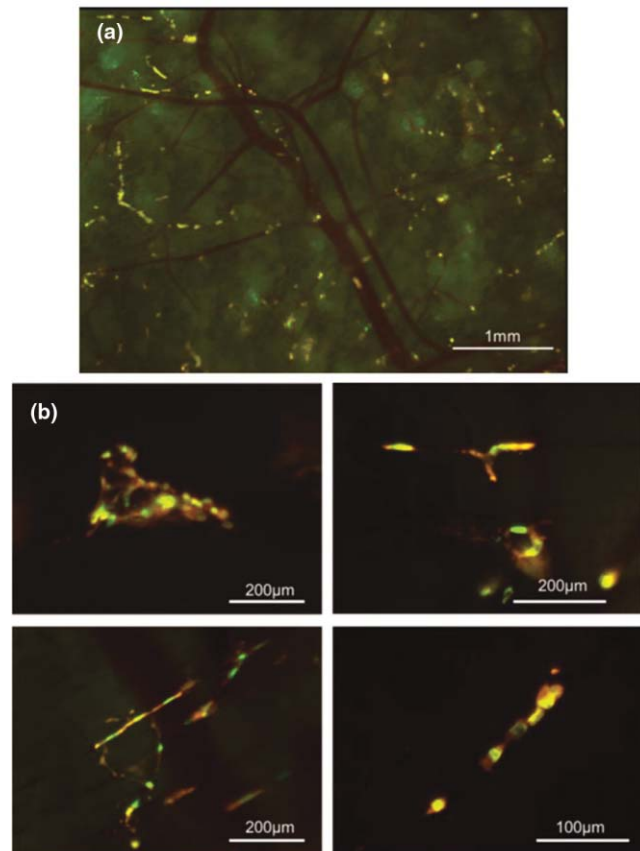
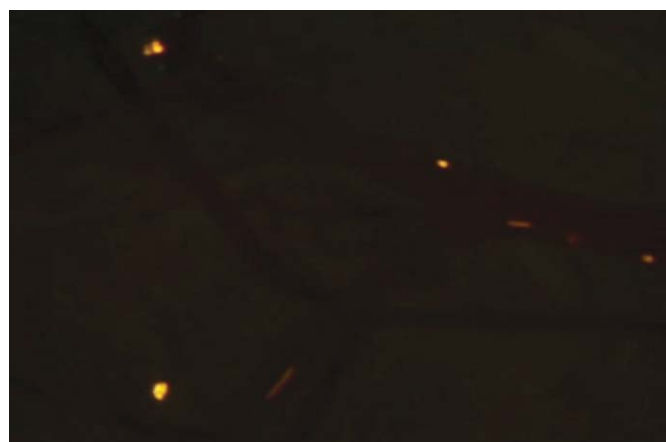


Fig. 4 Imaging trafficking cancer cells at the subcellular level. Visualization of 143B dual-color human osteosarcoma cells in microvessels and in capillaries on the skin in live mice. (a) Macroview: Immediately after 143B cell injection into epigastric cranialis vein, blood vessels and cells on the skin flap were imaged. Fluorescent cells were trapped in microvessels or capillaries and trafficked in larger vessels. See Video 1 of the trafficking cancer cells. (b) Microview: Some cells and nuclei were highly deformed and their morphology varied, depending on the diameter of the vessel. Cells were highly deformed, including their cytoplasm and nuclei, in order to fit a small-diameter capillary. These images were taken with a 2.0 \times objective lens.



Video 1 Trafficking cancer cells, labeled with GFP in the nucleus and RFP in the cytoplasm, in a blood vessels imaged with the MVX10. For details, see Fig. 4 (MPEG, 892 KB).
[URL: <http://dx.doi.org/10.1117/1.3526356.1>]

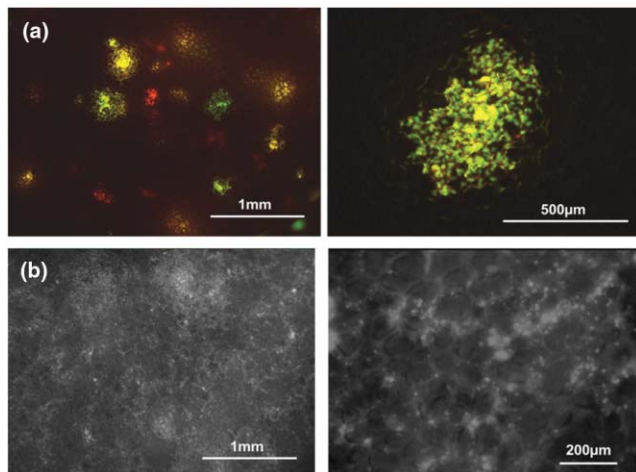


Fig. 5 Visualization of individual fluorescent cancer cells in lung of live mice. (a) Imaging of lung metastatic colonies of 143B dual-color human osteosarcoma cells. Two weeks after 2×10^6 dual-color 143B cell injection, the lung surface was imaged directly using the technique illustrated in Fig. 3(b). Lung metastatic colonies were visualized from the macro- to the subcellular level. At the macrolevel view, varied sizes and colors of metastatic colonies were observed. At the microlevel view, single cancer cells in a metastatic colony were observed. (b) Imaging of CFP splenocytes in lung. Six hours after CFP splenocytes were injected in the tail vein, the lung surface was imaged and CFP splenocytes remaining in the lung were visualized from macro to micro. All images in Fig. 5 were taken with $2.0 \times$ objective lens. (Color online only.)

3.2 Imaging of Metastases in the Lungs of Live Mice

We visualized lung metastatic colonies in live mice 2 weeks after 2×10^6 dual-color 143B cells were injected. Imaging was performed on mice with the chest wall opened using surgical and assisted ventilation procedures previously described and outlined here.⁹ Lung metastatic colonies were visualized from the macro to the subcellular level. At the macrolevel, varied sizes and colors of metastatic colonies were observed. The homogeneous color in each colony indicated that individual colonies developed from a single cancer cell. At the subcellular level, we could observe single cancer cells in the metastatic colonies. Most cells appeared viable, stably expressing^{10,11} both GFP and RFP [Fig. 5(a)].

3.3 Imaging Splenocytes of the Lung of Live Mice

We also imaged injected cyan fluorescent protein (CFP) expressing splenocytes in the lung, which were derived from the spleen of CFP transgenic mice and injected in the tail vein of mice being imaged.^{12,13} The CFP splenocytes of varying size were distributed heterogeneously on the lung surface [Fig. 5(b)].

We demonstrated that dynamic subcellular *in vivo* imaging is possible with the MVX10 using dual-colored cells. The nucleus and cytoplasm of individual cancer cells can be distinguished *in vivo*. This study focuses on intravital imaging of cancer cells on the surface of organs. Future studies will focus on deeper imaging. Cancer cells on organs, in addition to the lung, will be imaged and compared in future studies.

The main drawback of the MVX10 compared to the much more complex Olympus OV100 Small Animal Imaging System⁸ is the maximum magnification currently achievable. This may be improved in the future.

4 Conclusions

As demonstrated in this paper, the MVX10 fluorescence microscope is capable of *in vivo* fluorescence imaging from the macro- to the subcellular level in live mice. The images shown in this paper are comparable to the images obtained using the much more complex and expensive Olympus OV100 Small Animal Imaging System.⁸ The long-working-distance and very high light gathering capability of the high-NA objectives enable the MVX10 to visualize fluorescent-protein-labeled cells *in vivo* at very high resolution. With microscopes such as the MVX10 and use of fluorescent-proteins to stably label cells, organelles, and proteins, the new field of *in vivo* cell biology can become widely practiced in many areas of mouse-model research, including cancer, immunology, allergy, stem cells, infectious diseases, and many others.

References

1. R. M. Hoffman, "In vivo real-time imaging of nuclear-cytoplasmic dynamics of dormancy, proliferation and death of cancer cells," *Acta Pathol. Microbiol. Immunol. Scand.* **116**, 716–729 (2008).
2. R. M. Hoffman, "The multiple uses of fluorescent proteins to visualize cancer *in vivo*," *Nature Rev. Cancer* **5**, 796–806 (2005).
3. N. Yamamoto, P. Jiang, M. Yang, M. Xu, K. Yamauchi, H. Tsuchiya, K. Tomita, G. M. Wahl, A. R. Moossa, and R. M. Hoffman, "Cellular dynamics visualized in live cells *in vitro* and *in vivo* by differential dual-color nuclear-cytoplasmic fluorescent-protein expression," *Cancer Res.* **64**, 4251–4256 (2004).
4. P. Jiang, K. Yamauchi, M. Yang, K. Tsuji, M. Xu, A. Maitra, M. Bouvet, and R. M. Hoffman, "Tumor cells genetically labeled with GFP in the nucleus and RFP in the cytoplasm for imaging cellular dynamics," *Cell Cycle* **5**, 1198–1201 (2006).
5. A. Sakaue-Sawano, H. Kurokawa, T. Morimura, A. Hanyu, H. Hama, H. Osawa, S. Kashiwagi, K. Fukami, T. Miyata, H. Miyoshi, T. Imamura, M. Ogawa, H. Masai, and A. Miyawaki, "Visualizing spatiotemporal dynamics of multicellular cell-cycle progression," *Cell* **132**, 487–498, (2008).
6. M. Yang, E. Baranov, J-W. Wang, P. Jiang, X. Wang, F-X. Sun, M. Bouvet, A. R. Moossa, S. Penman, and R. M. Hoffman, "Direct external imaging of nascent cancer, tumor progression, angiogenesis, and metastasis on internal organs in the fluorescent orthotopic model," *Proc. Natl. Acad. Sci. U.S.A* **99**, 3824–3829 (2002).
7. M. Yang, P. Jiang, and R. M. Hoffman, "Whole-body subcellular multi-color imaging of tumor-host interaction and drug response in real time," *Cancer Res.* **67**, 5195–5200 (2007).
8. K. Yamauchi, M. Yang, P. Jiang, M. Xu, N. Yamamoto, H. Tsuchiya, K. Tomita, A. R. Moossa, M. Bouvet, and R. M. Hoffman, "Development of real-time subcellular dynamic multicolor imaging of cancer cell trafficking in live mice with a variable-magnification whole-mouse imaging system," *Cancer Res.* **66**, 4208–4214 (2006).
9. H. Kimura, K. Hayashi, K. Yamauchi, N. Yamamoto, H. Tsuchiya, K. Tomita, M. Bouvet, and R. M. Hoffman, "Real-time imaging of single cancer-cell dynamics of lung metastasis," *J. Cell. Biochem.* **109**, 58–64 (2010).
10. N. Yamamoto, M. Yang, P. Jiang, M. Xu, H. Tsuchiya, K. Tomita, A. R. Moossa, and R. M. Hoffman, "Determination of clonality of metastasis by cell-specific color-coded fluorescent-protein imaging," *Cancer Res.* **63**, 7785–7790 (2003).
11. N. Yamamoto, M. Yang, P. Jiang, M. Xu, H. Tsuchiya, K. Tomita, A. R. Moossa, and R. M. Hoffman, "Real-time imaging of individual fluorescent protein color-coded metastatic colonies *in vivo*," *Clin. Exper. Metast.* **20**(7), 633–638 (2003).

12. H. S. Tran Cao, H. Kimura, S. Kaushal, C. S. Snyder, J. Reynoso, R. M. Hoffman, and M. Bouvet, "The cyan fluorescent protein (CFP) transgenic mouse as a model for imaging pancreatic exocrine cells," *J. Panc.* **10**, 152–156 (2009).
13. H. S. Tran Cao, J. Reynoso, M. Yang, H. Kimura, S. Kaushal, C. S. Snyder, R. M. Hoffman, and M. Bouvet, "Development of the transgenic cyan fluorescent protein (CFP)-expressing nude mouse for Technicolor cancer imaging," *J. Cell. Biochem.* **107**, 328–334 (2009).